SUPPORTING MATERIAL

SILK FIBER MECHANICS FROM MULTISCALE FORCE DISTRIBUTION ANALYSIS

Murat Cetinkaya, Senbo Xiao, Bernd Markert , Wolfram Stacklies, Frauke Gräter

SUPPORTING METHODS

All-atom Molecular Dynamics (MD) simulations

All MD simulations were performed with Gromacs 4.0.5 (27). For force distribution analyses, an extension of Gromacs (38) was utilized to write out atomic pair-wise forces. The simulation parameters were the same as in the previous study (9). Shortly, the OPLS-AA force field (28) for the protein and the TIP4P model (29) for water were employed, a time step of 2 fs was used, and simulations were performed at constant temperature (300 K) and pressure (1 bar), with periodic boundary conditions and with Particle-Mesh Ewald summations for long-range (>1 nm) electrostatics (39). All simulations were run without any bias regarding force field parameters or boundary conditions.

Crystalline subunit. The all-atom model is composed of five layers, each layer containing five β-strands with each β-strand having eight alanine repeats. Details on the modeling, equilibration, and force distribution analysis of the crystalline subunits have been published (9). The crystalline subunit was totally intact throughout the equilibration and up to the rupture point in the force-probe simulations. Supporting Fig. S5 shows the RMSD of the β-sheets in a crystalline subunit during an equilibrium MD simulation. The overall RMSD is as low as ~0.11 nm after 10 ns.

Amorphous subunit. The all-atom model comprises the 24 residue sequence known to form the amorphous subunit in *Araneus diadematus* spider silk (GPGGYGPGSQGPSG PGGYGPGGPG, where G, P, Y, S, Q are glycine, proline, tyrosine, serine, and glutamine, respectively). A single peptide chain was generated in a partially extended conformation (end-to-end distance of 6.2 nm), solvated in water with physiological ion concentration (100 mM), resulting in a system of 6x6x10 nm^3 and ~47000 atoms. During 20 ns of equilibrium MD simulations, the chain collapsed to an average distance of 0.38 nm. To obtain a force-extension curve with minimal nonequilibrium effects, we used umbrella sampling, in which harmonic potentials acted on the peptide termini along *z*-direction. We sampled in 34 windows for 20 ns each, starting from snapshots with varying the end-to-end distances (0.12 to 8.87 nm). The harmonic potential force constant was 100 kJ/mol/nm^2. All other simulation parameters were kept the same as in the all-atom simulations of the crystalline subunit. Weighted histogram analysis method (40) was applied to check the overlap between the umbrella samples and to calculate the stretching force of the peptide as a function of its end-to-end distance.

Composite unit. Two crystalline subunits were serially coupled with an amorphous subunit and pulled away from each other. The amorphous subunit was composed of eight entangling peptide chains having 50% initial extension relative to the chain contour length. This initial extension was chosen as an intermediate value of a polymer in shear flow (see e.g. Rammensee, et al. (8)), as it is present in the spider gland during silk fiber spinning. In natural spider silk fibers, cross

linking of the crystalline units via disordered chains occurs randomly to an extent that depends on the alignment of the chains during fibrillogenesis due to shear flow. Our model corresponds to a situation where approximately one third of the disordered peptide chains (8 out of 25) connected the same crystalline subunit to another one. Conformations for the disordered peptide chains at an extension of 50% of the contour length were taken from umbrella sampling MD simulations (see above). The strands from the two crystals were connected by the eight peptide chains as shown in Fig. 3b in the main text. For the skeleton model, we find the connectivity not to influence the effective elastic response of the composite unit. Probing a composite unit with different connectivity (e.g. with all straight chains) is computationally demanding, and can be expected to also give a similar elastic response, given the efficient cross-chain force distribution (see Results in the main text). The composite unit was solvated with TIP4P water in a 7x7x45 nm^3 box with 100 mM ion concentration. The system had a total number of ~300,000 atoms. After energy minimization using steepest descent method, 500 ps position restrained simulations were followed by 10 ns equilibrium simulations. As a further validation of the all-atom model, the density of the composite unit was calculated as 1.12 g/cm^3, in good agreement with ~1.14 g/cm^3, calculated by Fossey (11) and in reasonable agreement with the experimental results for similar silk fibers with ~1.35 g/cm^3 (41) and for the amorphous regions with ~1.14 g/cm^3 (42). To obtain a force-elongation curve, crystalline subunits were pulled using virtual springs with harmonic force constants (500 $kJ/mol/nm^2$) acting at the center of mass of the alanines at the C and N-termini of the composite unit. The springs were moved away from each other with a velocity of 0.2 m/s. The force-probe MD simulations were stopped after rupture occurred at ~60 ns. For the force distribution analysis, constant forces of 1600 kJ/mol/nm and 100 kJ/mol/nm were applied to the same pulling groups to sample the perturbed and relaxed states, respectively. The system was equilibrated under this constant force and the pairwise forces in the composite unit were averaged and written out over 10 ps intervals. For both states, five independent MD simulations (10 ns each) were performed and the pairwise forces averaged over the aggregated simulation time. All other parameters were identical to those described above.

Finite Element (FE) simulations of the skeleton and comprehensive fiber models

Crystalline subunit. We constructed a skeleton model of the crystalline subunit (5x5 β-strands) consisting of four types of isotropic Euler beams. Each protein backbone was represented by a single elastic member. We defined a linear elastic modulus, E, of ~743.0 GPa as obtained from stretching a single $(Ala)_8$ chain in force-probe MD simulations. For other members, representing single covalent bonds (i.e. C=O, N-H, and C_α-C_β), the elastic modulus was directly obtained from the force constant k of these bonds in the OPLS/AA force field (28), using $E=kL_0A_o^{-1}$, resulting in ~297.0 GPa. The nominal cross sectional area A_o was calculated by assuming a bond radius of 0.1 nm for all covalently bonded members. Similar to the covalent bonds, the nonbonded interactions between alanine side-chain (CH_3) groups in the all-atom model were also represented with linear elastic members in the skeleton model. These members connected backbone members between β-sheet layers. The elastic response was estimated from a Lennard-Jones (LJ) potential fitted to the total interaction energy between alanine CH_3 groups in equilibrium MD simulations. Nominal length of the corresponding members in the skeleton model, L_0, was the equilibrium CH_3-CH_3 distance observed in MD simulations.

Hydrogen bonds in the crystalline subunit, connecting the backbone members within a β-sheet layer, were represented with nonlinear elastic members in order to consider the weakening of hydrogen bonds with increasing strain. The strain-dependent elastic modulus of the hydrogen

bonds was calculated from the first derivative of the hydrogen bond potential, defined as the sum of the Lennard-Jones and Coulomb interactions between the four atoms taking part in hydrogen bonding (i.e., N-H and C=O) as defined by the OPLS-AA force field (28). The cross sectional radius of the members representing the nonbonded interactions (intrasheet hydrogen bonds and intersheet side-chain interactions) was taken as 0.06 nm (details provided in Xiao, et al. (9)). Nominal length, L_0, of the members representing the hydrogen bonds was defined as the equilibrium hydrogen bond (O···H) distance observed in MD simulations.

Amorphous subunit. The amorphous subunit was modeled with nonlinear elastic members, each of which corresponds to a 24-mer peptide chain as in the all-atom model. The force elongation curve of the amorphous chain from all-atom MD simulations (see above) was used as an input for the skeleton model. The elastic modulus increases with chain length L, as a result of the entropic stiffening characteristic for polymer chains (Supporting Fig. S3a). This mechanical behavior was observed at different portions of umbrella sampling MD simulations, indicating that the simulation time scale was not a major limitation (Supporting Fig. S3b). At low forces the convergence between force-extension curves is reasonable, and at higher forces the curves overlap. The cross sectional radius of the corresponding members in the skeleton model was 0.1 nm as for other covalent members, and nominal member length, L_0, was taken as 0.38 nm, which was the average end-to-end distance of the coiled peptide chain during equilibration MD simulations.

Composite unit. Analogous to the all-atom composite unit, we serially coupled two crystalline subunits with an amorphous subunit consisting eight diagonally oriented chains. External tensile stress was applied in a distributed manner at the termini of each crystal in opposite directions. Parameters of the members in the composite unit were same as in the skeleton models of the individual subunits.

Comprehensive fiber model. This model was only tested with FE simulations, since MD simulations of the same system at atomistic scale (~ 1.2 million atoms) were computationally unfeasible. A three dimensional solid stress-strain model was used for the fiber FE simulations. Amorphous subunits were assumed to be completely isotropic (E_a = 2.7 GPa) while the crystalline subunits were modeled as transversely isotropic (E_c = 80.0 GPa in the pulling direction). The elastic moduli of the subunits were calculated from the all-atom simulations of the composite unit. Poisson's ratio for both types of subunits was taken as ~0.33 in the pulling direction, as suggested by Fossey for poly(Gly-Ala) crystals (11). These values were used as input for the comprehensive fiber model. The fiber was represented by a linear elastic cylindrical solid member pulled by distributed loads acting on both ends. The fiber was 7 nm in radius and 39 nm in length. The crystalline subunits were represented with linear elastic cubic members 12 nm^3 in size, corresponding to the dimensions of the all-atom crystalline subunit, and embedded into a continuous amorphous phase without any slip at the interfaces. We compared a random distribution state of the crystals in the fiber with two other extreme states, named as serial (lamellar) and parallel (longitudinal) distribution of the crystals. We note that the parallel distribution, even though insightful for comparison, cannot be realized due to the block-copolymer like silk protein sequence. The elastic modulus of the fiber, E_f, was determined with varying crystallinity, which is the volume percentage of the crystals in the fiber (Fig. 4a in the main text). Rupture strength and strain of the fiber were estimated from the stress distribution analysis across the fiber (Fig. 4b in the main text). More precisely, the fiber's rupture stress and strain were the values at the instant where the average tensile stress in the crystalline subunits reached 2.0 GPa. This was the value observed in the all-atom model of the composite unit prior

to rupture. Toughness, the integral of the stress-strain curve, of the fiber was calculated as half the product of the rupture stress and the strain based on our definition. We here do not take yielding of the fiber into account, which allows for a further increase in (plastic) strain without the failure of the fiber. We thus consider the estimated rupture strain and toughness values to present the lower limits of the actual rupture strain and toughness, respectively.

REFERENCES

38. Stacklies, W., M. C. Vega, M. Wilmanns, and F. Graeter. 2009. Mechanical network in titin immunoglobulin from force distribution analysis. *PLoS Comput. Biol.* 5: e1000306.
39. Darden, T., D. York, and L. Pedersen. 1993. Particle mesh Ewald-an Nlog(N) method for Ewald sums in large systems. *J. Chem. Phys.* 98: 10089-10092.
40. Kumar, S., J. M. Rosenberg, D. Bouzida, R. H. Swendsen, and P. A. Kollman. 1992. The weighted histogram analysis method for free-energy calculations on biomolecules. I. The method. *J. Comput. Chem.* 13: 1011-1021.
41. Guess, K. B., and C. Viney. 1998. Thermal analysis of major ampullate (drag line) spider silk: the effect of spinning rate on tensile modulus. *Thermochim. Acta.* 315: 61-66.
42. Saravanan, D. 2006. Spider Silk – Structure, Properties and Spinning. *Journal of Textile and Apparel, Technology and Management.* 5:1-20.

SUPPORTING FIGURE LEGENDS

Supporting Figure S1. Pull-out resistance of the crystalline subunit. Results from the all-atom (*black*) and skeleton models (*red*) as the middle strand is pulled out from the crystalline subunit (*indicated by the red β-strand in the lower inset*). A linear fit for the all-atom model is shown with blue line. The upper inset shows the pull-out resistance-strain curves for a higher range of values.

Supporting Figure S2. Distribution of the pulling force (1.66 nN) in the crystalline subunit. Pulling force is applied to the central strand and the responses from the skeleton (a) and all-atom (b) models are shown. Only the axial forces in the backbone are shown as color codes. The strands in (b) are shown in cartoon representation.

Supporting Figure S3. Mechanical behavior of the disordered peptides in the amorphous subunits. (a) Elastic modulus of the members representing the disordered chains of the amorphous subunit in the skeleton model. The nonlinear behavior of these chains resembles a neo-Hookean solid. Up to a certain chain length, a constant value of 1.6 GPa was used for convenience. The upper limit was set as 743.0 GPa, which is the elastic modulus value for the fully extended backbone members. Schematics represent the state of chain extension. (b) Force-extension curves of a disordered peptide chain obtained from different portions of umbrella sampling MD simulations. At low forces the convergence between force-extension curves is reasonable, and at high forces the curves overlap indicating full convergence.

Supporting Figure S4. Stress-strain curve of the amorphous subunits in the absence of the crystalline subunits in an all-atom model. Inset shows the schematic of the pulling process.

Supporting Figure S5. RMSD of a crystalline subunit during an equilibrium MD simulation of 10 ns. The overall RMSD of all 25 β-sheets in the crystalline subunit (black) is shown along with the RMSD regarding the inner 9 (red) and outer 16 β-sheets (blue).

SUPPORTING FIGURES

S1.

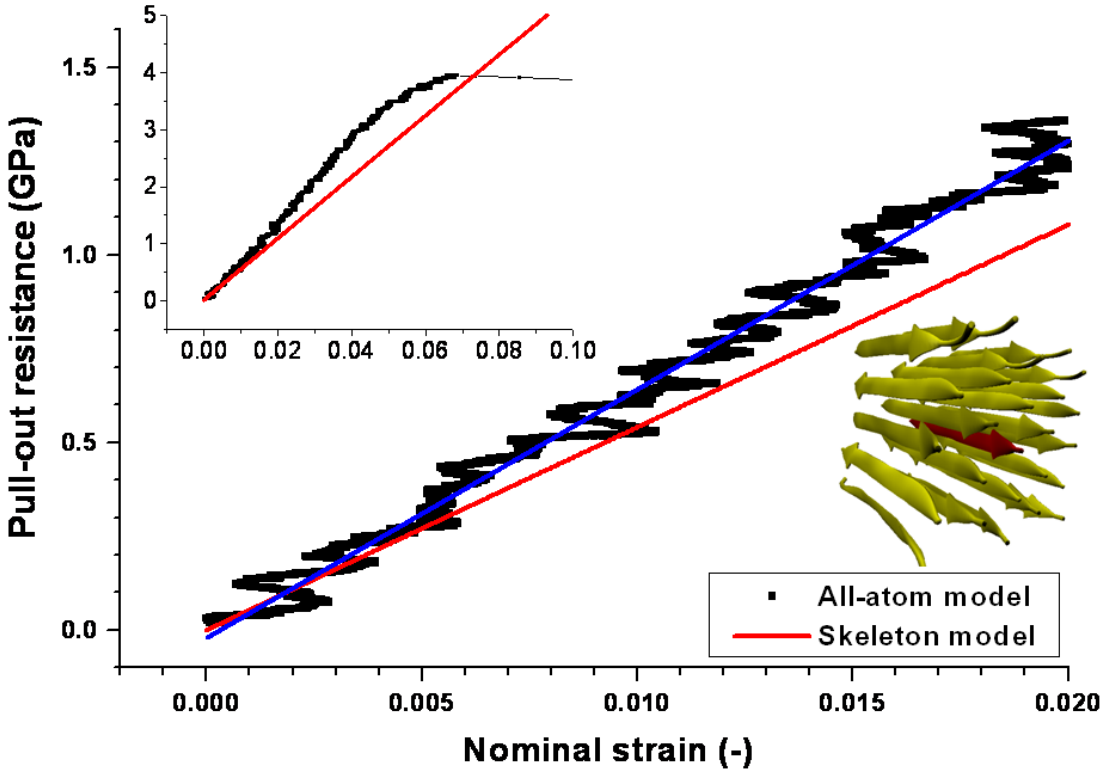

S2.

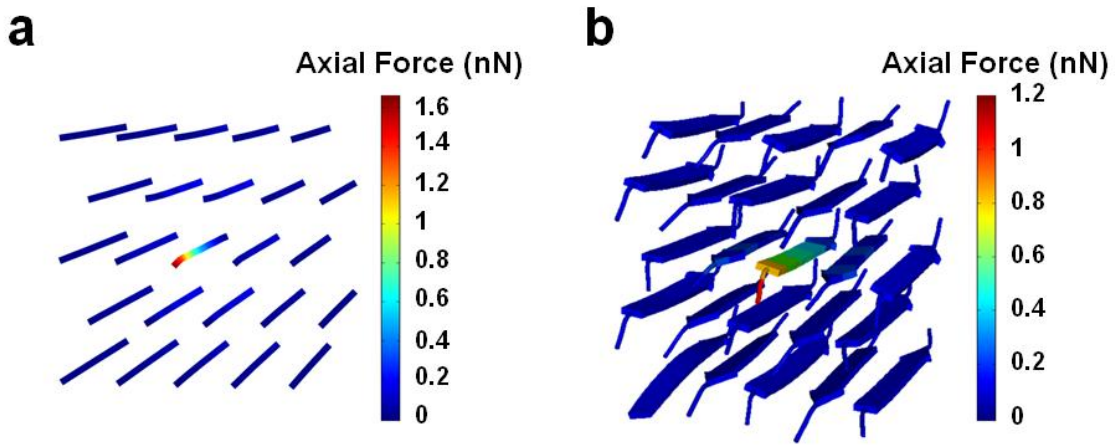
a
Axial Force (nN)
1.6
1.4
1.2
1
0.8
0.6
0.4
0.2
0
b
Axial Force (nN)
1.2
1
0.8
0.6
0.4
0.2
0

S3.

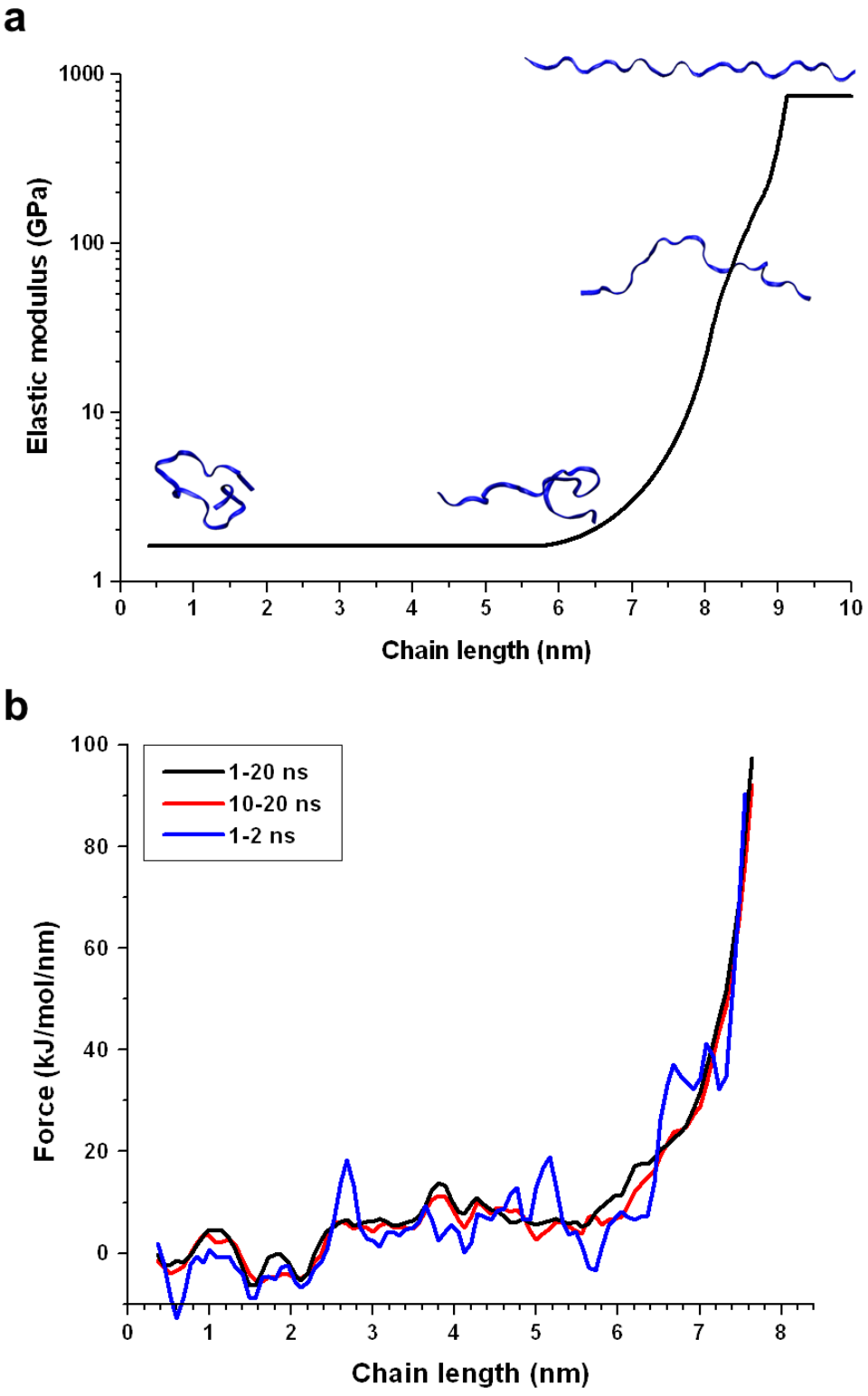
a
Elastic modulus (GPa)
1000
100
10
1
0
1
2
3
4
5
6
7
8
9
10
Chain length (nm)
b
Force (kJ/mol/nm)
100
80
60
40
20
0
1-20 ns
10-20 ns
1-2 ns
0
1
2
3
4
5
6
7
8
Chain length (nm)

S4.

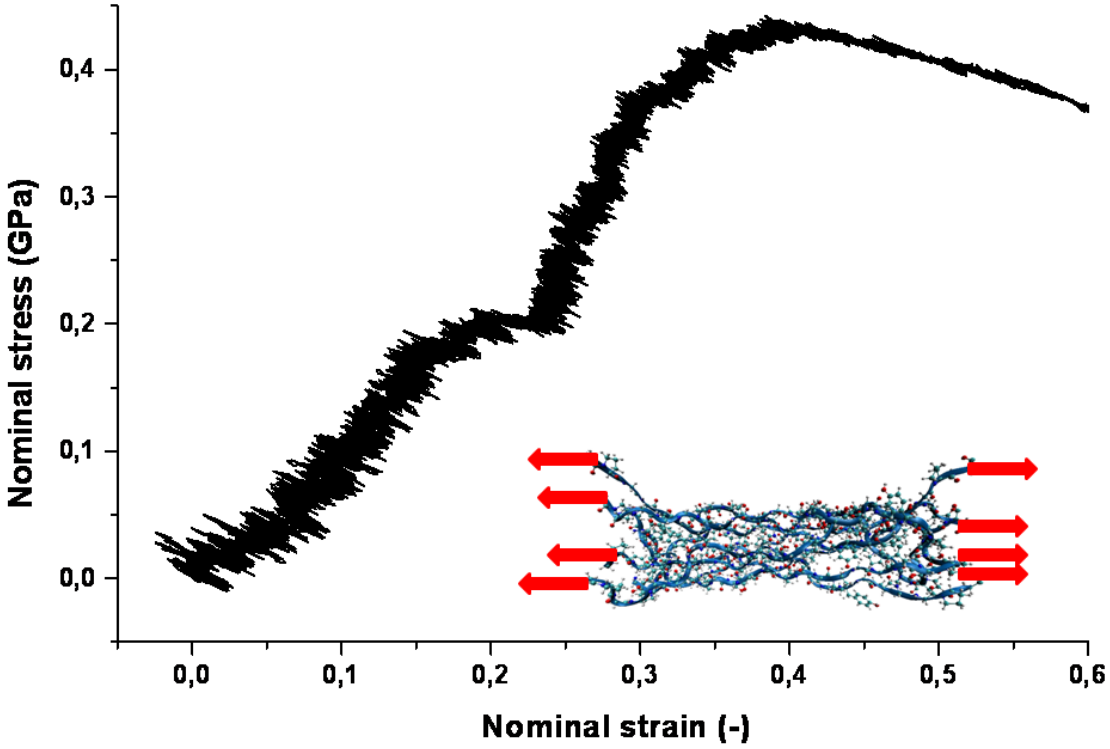
Nominal stress (GPa)
0,0
0,1
0,2
0,3
0,4
0,0
0,1
0,2
0,3
0,4
0,5
0,6
Nominal strain (-)

S5.

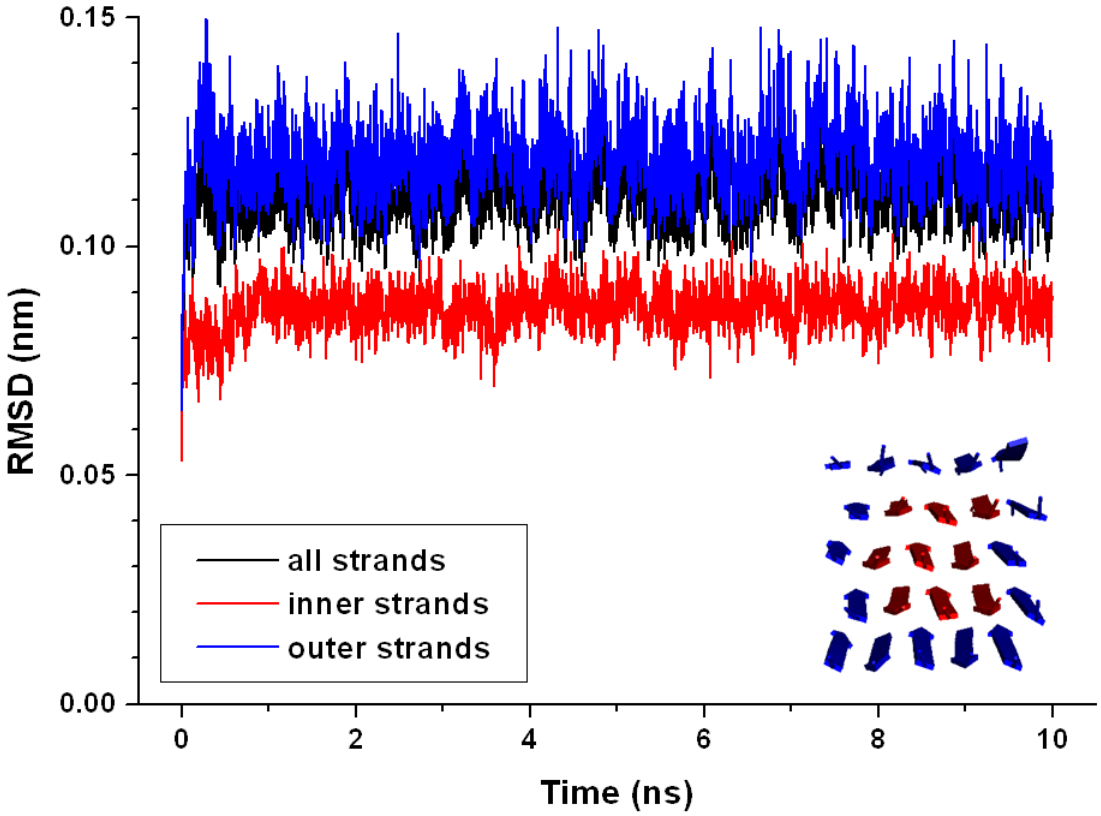
0.15
0.10
0.05
0.00
RMSD (nm)
0
2
4
6
8
10
Time (ns)
all strands
inner strands
outer strands